NACA RM L50D05

NACA

RESEARCH MEMORANDUM

AERODYNAMIC CHARACTERISTICS AT A MACH NUMBER OF 1.25 OF A 6-PERCENT-THICK TRIANGULAR WING AND 6- AND 9-PERCENT-THICK TRIANGULAR WINGS IN COMBINATION WITH A FUSELAGE

WING ASPECT RATIO 2.31, BICONVEX AIRFOIL SECTIONS

By Albert W. Hall and Garland J. Morris

Langley Aeronautical Laboratory
Langley Air Force Base, Va.

NATIONAL ADVISORY COMMITTEE
FOR AERONAUTICS

WASHINGTON

May 5, 1950

NACA RM L50D05

NATIONAL ADVISORY COMMITTEE FOR AERONAUTICS

RESEARCH MEMORANDUM

AERODYNAMIC CHARACTERISTICS AT A MACH NUMBER OF 1.25 OF A 6-PERCENT-THICK TRIANGULAR WING AND 6- AND 9-PERCENT-THICK TRIANGULAR WINGS IN COMBINATION WITH A FUSELAGE

WING ASPECT RATIO 2.31, BICONVEX AIRFOIL SECTIONS

By Albert W. Hall and Garland J. Morris

SUMMARY

Tests were made at a Mach number of 1.25 by the wing-flow method to determine the aerodynamic characteristics of two semispan delta-wing configurations. One configuration was a 6-percent-thick biconvex wing tested alone and in combination with a fineness-ratio-12 fuselage and the other was a 9-percent-thick biconvex wing in combination with the fuselage. Both wings had as aspect ratio of 2.31 (half-apex angle of 30°).

Measurements were made of normal force, chord force, and pitching moment for various angles of attack. The Reynolds number of the tests was approximately 8.8×10^5 based on mean aerodynamic chord of wing alone.

A comparison of results for the 6-percent-thick wing alone and in combination with the fuselage indicated that the variation of lift coefficient with angle of attack and of drag coefficient with lift coefficient was very nearly the same for the two arrangements if the coefficients for the combination were based on the wing area extended to the fuselage center line. On the same basis, the aerodynamic center of the wing-fuselage combination was about 3 percent mean aerodynamic chord farther forward than for the wing alone. The drag at zero lift for the combination was approximately equal to the sum of the drag of the isolated wing (of the same area as the exposed wing area of the combination) and the drag of the fuselage alone.

Increasing the thickness of the wing of the wing-fuselage combination had little effect on the lift, pitching moment, or variation of drag with lift. The drag at zero lift of the 9-percent-thick wing including wing-fuselage interference (that is, wing-fuselage drag less fuselage drag) was about 85 percent greater than that of the 6-percent-thick wing including wing-fuselage interference.

INTRODUCTION

As part of a program to determine the effect of leading-edge sweep, wing section, and thickness on the aerodynamic characteristics of delta wings at transonic and low-supersonic speeds, wing-flow tests were made of a 6-percent-thick biconvex wing alone and in combination with a fuselage, and of a 9-percent-thick biconvex wing in combination with a fuselage. Both wings had an aspect ratio of 2.31 (half-apex angle of 30°). Normal force, chord force, pitching moment, and angle of attack were measured for each configuration at Mach numbers in the range 1.21 to 1.29. The results are presented only for a Mach number of 1.25. The test Reynolds number was 8.8×10^5 ±6 percent based on the mean aerodynamic chord of the wing alone.

SYMBOLS

M_o	airplane flight Mach number
M_L	local Mach number at surface of test section
M	effective Mach number at wing of model
C_{L_a}	airplane lift coefficient
q	effective dynamic pressure at wing of model, pounds per square foot
R	Reynolds number based on mean aerodynamic chord of model
ϵ	half-apex angle of model wing, degrees
α	angle of attack of model wing, degrees
S	semispan wing area of model, square feet
b	span of wing, inches

c	local wing chord, inches
$\bar{c}$	mean aerodynamic chord of model wing, inches $\left(\frac{\int_0^{b/2} c^2 \, db}{\int_0^{b/2} c \, db}\right)$
L	lift, pounds
M	pitching moment about 50 percent $\bar{c}$ point, inch-pounds
D	drag, pounds
C_L	lift coefficient $\left(\frac{L}{qS}\right)$
C_m	pitching-moment coefficient $\left(\frac{M}{qS\bar{c}}\right)$
C_D	drag coefficient $\left(\frac{D}{qS}\right)$
$C_{D_{min}}$	minimum drag coefficient
$\frac{dC_L}{d\alpha}$	rate of change of lift coefficient with angle of attack
A	aspect ratio $(4 \tan \epsilon)$

APPARATUS AND TESTS

The tests were made by the NACA wing-flow method in which the model was mounted in a region of high-speed flow over the wing of an F-51D airplane (fig. 1).

The contour of the airplane wing in the test region was different from that used in previous wing-flow investigations in that it was designed to give a uniform velocity field at Mach numbers near 1.25 rather than through the transonic range.

The semispan-model configurations tested were: 6-percent-thick biconvex wing with each of two end plates; the same 6-percent-thick

biconvex wing in combination with a fuselage with exposed wing area equal to the area of the wing alone; 9-percent-thick biconvex wing in combination with a fuselage; and a fuselage alone. An investigation was also made on the 6-percent-thick wing in presence of the small end plate, but detached from it to determine the tare of the small end plate. The space between the wing and the end plate was about 0.005 inch.

Both delta wings had an aspect ratio of 2.31 ($\epsilon = 30^{\circ}$). The fuselage was a half-body of revolution of fineness ratio 12 and was equipped with an end plate. Both fuselage and end plate were curved to conform to the contour of the airplane wing surface in the test region. Details of the various configurations are presented in figures 2 and 3 and in tables I and II. The fuselage used for the 9-percent-thick wing-fuselage test had been altered slightly following the tests of the 6-percent-thick wing-fuselage and the fuselage alone. When the 9-percent-thick wing-fuselage configuration was tested, there was a hole in the rear portion of the fuselage which was partially filled by a shaft extending to the fuselage surface. (The location of the hole is shown in fig. 3.) The models were mounted about 1/64 inch above the surface of the test section and fastened to a strain-gage balance below the test section by means of a shank which passed through a hole in the test section.

The chordwise distribution of local Mach number M_L along the airplane wing surface in the test region is shown (relative to the model location) in figure 4 for several values of airplane Mach number M_o and lift coefficient C_{L_a}. The local Mach number was determined from static-pressure measurements made with orifices flush with the surface in tests with the model removed. The variation of Mach number with distance above the surface was determined from static-pressure measurements made with a static-pressure tube located at various distances above the surface of the test section; the vertical Mach number gradient was found to be 0.009 per inch up to a distance of 6 inches above the surface. The effective Mach number M at the wing of the model was determined as an average Mach number over the area of the model. The range of effective Mach numbers for these tests was 1.21 to 1.29; the lower limit is due to the passing of a compression shock over the model location at an effective Mach number less than 1.21 and the upper limit of 1.29 is determined by the airplane Mach number at which the airplane may be safely operated. The boundary-layer thickness in the test region was found to be about 0.25 inch.

A free-floating vane mounted outboard of the model station (fig. 1) was used to determine the direction of local air flow. The flow angle at the model station was calibrated against the flow angle at the outboard vane by mounting a similar vane at the model station, first 7.8 inches and then, 13.3 inches behind 33 percent chord of the F-51D wing.

(See fig. 4 for the relationship of these points to the model location.) A flow-angle difference between these two chord points of about 1° was apparently due to a small spanwise pressure gradient. The local air flow was determined by interpolation of these data to give the local flow at a point near the center of the exposed-model wing area.

The tests were made in high-speed dives of the F-51D airplane. Measurements were made of angle of attack, normal force, chord force, and pitching moment as the effective Mach number was increased from 1.21 to 1.29 and as the model was oscillated through an angle-of-attack range of -3° to 12° for the wing alone and -5° to 9° for the wing-fuselage combination. The Reynolds number was 8.8×10^5 ±6 percent based on the mean aerodynamic chord of the model wing alone.

DISCUSSION OF RESULTS

The results are presented only for a Mach number of 1.25, since there did not appear to be any significant variation in characteristics over the small Mach number range covered in the tests.

The coefficients for the wing-fuselage configurations were based on the wing area extended to the fuselage center line as shown in figure 3. The method used is in agreement with that used in other investigations.

Lift Characteristics

The variation of C_L with angle of attack for the wing alone and wing-fuselage models is shown in figure 5. The curves for the 6-percent-thick wing with either the large end plate, the small end plate, or the fuselage indicate little or no effect of end-plate size or of the addition of a fuselage. The points shown for the 6-percent-thick wing in the presence of, but detached from, the small end plate show a slight loss of lift at higher angles. This loss is probably the result of leakage between the wing and end plate (gap between wing and end plate was approx. 0.005 inch). Hereinafter C_L of the 6-percent-thick wing alone will refer to the curve for the wing with end plate attached. The 6-percent-thick wing alone had a maximum lift coefficient of 0.54 at 11.3° angle of attack. At zero lift coefficient, the rate of change of lift coefficient with angle of attack $\left(\frac{dC_L}{d\alpha}\right)_{L=0}$ was approximately 0.047 per degree for all configurations as compared to the theoretical

value of 0.054 per degree (reference 1). The value of $\frac{dC_L}{d\alpha}$ increased with increasing C_L for all of the 6-percent-thick wing configurations, but remained essentially constant at 0.046 per degree for the 9-percent-thick wing-fuselage configuration. The angle of attack for zero lift was slightly negative for all configurations, possibly as a result of the previously mentioned flow curvature at the model station.

Drag Characteristics

The variation of C_D with C_L^2 for the 6-percent-thick wing detached from the small end plate, the 6-percent-thick wing-fuselage combination, and the 9-percent-thick wing-fuselage combination is shown in figure 6. Since the variation of C_D with C_L^2 was linear for both the 6- and 9-percent-thick wing-fuselage models, it seemed reasonable to assume a similar variation for the 6-percent-thick wing detached from the small end plate. Because of a lack of intermediate points, the C_D curves for the 6-percent-thick wing detached from the small end plate are indicated by dashed lines. The drag variation with lift is practically the same for the three arrangements. It will be noted that the slope of the curves $\frac{dC_D}{dC_L^2}$ (about 0.34) is only slightly less than the inverse of the lift-curve slope $\frac{dC_L}{d\alpha}$ (fig. 5) in radians, indicating that the resultant force due to angle of attack was acting very nearly normal to the chord plane. This value of $\frac{dC_D}{dC_L^2}$ is almost twice the theoretical value computed from reference 1.

The drag coefficient at zero lift of the wing-fuselage combination less fuselage - that is, the drag of the wing including wing-fuselage interaction effects - was found to be 0.013 for the 6-percent-thick wing and 0.024 for the 9-percent-thick wing (figs. 6 and 7) representing an increase of about 85 percent due to the increase in wing thickness. According to theory (reference 2), the ratio of the wave drag of the 9-percent-thick wing to the 6-percent-thick wing is equal to the ratio of the square of the corresponding thickness ratios (that is, 2.25). Assuming a skin-friction drag coefficient of 0.006 and reducing this to 0.0045 (by the ratio of the exposed area to the total area), the wave drag ratio is 2.29.

The variation of C_D with angle of attack for the 6-percent-thick wing separated from the end plate, the fuselage alone with end plate, the 6-percent-thick wing-fuselage combination, and the wing alone plus

fuselage alone is shown in figure 7. The drag coefficient for the wing alone is based on a semispan area of 8 square inches while the C_D for the fuselage alone with end plate and the wing-fuselage combination is based on the semispan area of the wing extended to the fuselage center line, 10.78 square inches (fig. 3). The curve for the 6-percent-thick wing plus the fuselage was obtained as follows:

$$C_{D_{total}} = \left(\frac{8}{10.78} C_{D_o} + C_{D_i}\right) + C_{D_{fuselage}}$$

where

C_{D_o} drag coefficient at zero lift of 6-percent thick wing separated from end plate

C_{D_i} drag coefficient due to lift of 6-percent-thick wing separated from end plate

$C_{D_{fuselage}}$ drag coefficient of fuselage alone at corresponding angle of attack

The resulting curve is very close to the curve for the wing-fuselage combination and therefore shows very little interference effect. The drag of the fuselage alone with end plate should not be considered as representing the fuselage-alone drag because the end plate probably contributes an appreciable part of the measured values and a large portion of the fuselage is immersed in the boundary layer of the test section. Wing-fuselage interaction effects, however, are believed to be reliably reproduced.

Pitching-Moment Characteristics

The variation of C_m with C_L for the 6-percent-thick wing alone and the 6- and 9-percent-thick wing-fuselage configurations is shown in figure 8. The pitching-moment coefficients are taken about the 50-percent mean-aerodynamic-chord point for the wing alone and the 50-percent mean-aerodynamic-chord point of the wing extended to the fuselage center line for the wing-fuselage configuration. The small differences shown between the points for the 6-percent-thick wing in the presence of, but separated from, the small end plate, the curve for the same wing attached to the small end plate, and the curve for the same wing attached to the large end plate are probably within the accuracy of the measurements and not indicative of the effects of end plate or end-plate size. The curve for the wing-fuselage configuration shows that within the scope of the data C_m is not appreciably affected by increasing the wing thickness from

6 to 9 percent. At low lift coefficients $(C_L = 0.1)$, the aerodynamic center for the wing alone is located near the $0.48\bar{c}$ point and moves forward to the $0.45\bar{c}$ point as the C_L increases to 0.4. At low lift coefficients $(C_L = 0.1)$, the aerodynamic center for the wing-fuselage configurations is near the $0.45\bar{c}$ point (based on $\bar{c}$ of wing extended to the fuselage center line) and moves forward to the $0.42\bar{c}$ point at $C_L = 0.4$. While the location of the aerodynamic center is different for the wing alone and the wing-fuselage configurations, the amount of travel is the same (that is, about 3 percent $\bar{c}$).

The variation of C_L and C_m with angle of attack for the fuselage alone with end plate is shown in figure 9. The coefficients are based on the semispan area and mean aerodynamic chord of the wing extended to the fuselage center line. The value of $\frac{dC_m}{d\alpha}$ for the fuselage alone is about the same as that for the wing-fuselage combination; hence it appears that the effective aerodynamic center of the wing extended to the fuselage center line is at 50 percent $\bar{c}$.

Comparison with Other Results

A comparison of $\frac{dC_L}{d\alpha}$ and $C_{D_{min}}$ for the 6-percent-thick wing alone with wind-tunnel data given in reference 3 is shown in figure 10. The wing used for the wind-tunnel tests was a full-span delta wing of aspect ratio 2 with a 5-percent-thick double-wedge section having the maximum thickness at the midchord point. While the lift-curve slope seems to show good agreement between the wing-flow test and the wind-tunnel test, the difference in aspect ratio must be considered. By the wing-flow method, the lift-curve slope is 87 percent of the theoretical value while the lift-curve slope given by the wind-tunnel test is about 95 percent of the theoretical value ($M = 1.25$). In comparing the minimum drag coefficient, it should be noted that the wind-tunnel tests have not been corrected for the effects of the support body.

CONCLUDING REMARKS

Tests made by the NACA wing-flow method on two wing-fuselage models with delta wings of aspect ratio 2.31 and 6- and 9-percent-thick biconvex sections, and on the 6-percent-thick wing alone indicate these results at a Mach number of 1.25.

The variation of lift coefficient with angle of attack and of drag coefficient with lift coefficient was very nearly the same for the 6-percent-thick wing alone and in combination with the fuselage if the coefficients for the combination were based on the wing area extended to the fuselage center line. On the same basis, the aerodynamic center of the wing-fuselage combination was about 3 percent mean aerodynamic chord farther forward than for the wing alone. The drag at zero lift for the combination was approximately equal to the sum of the drag of the isolated wing (of the same area as the exposed wing area of the combination) and the drag of the fuselage alone.

Increasing the thickness of the wing of the wing-fuselage combination had little effect on the lift, pitching moment, or variation of drag with lift. The drag at zero lift of the 9-percent-thick wing including wing-fuselage interference (that is, wing-fuselage drag less fuselage drag) was about 85 percent greater than that of the 6-percent-thick wing including wing-fuselage interference.

Langley Aeronautical Laboratory
National Advisory Committee for Aeronautics
Langley Air Force Base, Va.

REFERENCES

1. Brown, Clinton E.: Theoretical Lift and Drag of Thin Triangular Wings at Supersonic Speeds. NACA Rep. 839, 1946.

2. Puckett, Allen E.: Supersonic Wave Drag of Thin Airfoils. Jour. Aero. Sci., vol. 13, no. 9, Sept. 1946, pp. 475-484.

3. Love, Eugene S.: Investigations at Supersonic Speeds of 22 Triangular Wings Representing Two Airfoil Sections for Each of 11 Apex Angles. NACA RM L9D07, 1949.

TABLE I

GEOMETRIC CHARACTERISTICS OF MODEL CONFIGURATIONS

Wing Alone:	
Section	biconvex
Thickness ratio, percent chord	6
Half-apex angle, degrees	30
$\bar{c}$, inches	3.51
Semispan area, square inches	8.0
Aspect ratio	2.31
Fuselage:	
Section	modified 65-series body of revolution
Length, inches	14.0
Maximum diameter at 50 percent length, inches	1.17
Fineness ratio	12
Wing and Fuselage Combination:	
Section	biconvex
Thickness ratio, percent chord	(1) 6 (2) 9
Semispan wing area including projected area of wing in fuselage, square inches	10.78
$\bar{c}$, inches	4.07
Dihedral, degrees	0
Incidence, degrees	0

TABLE II

ORDINATES FOR FUSELAGE

[All dimensions are in in.]

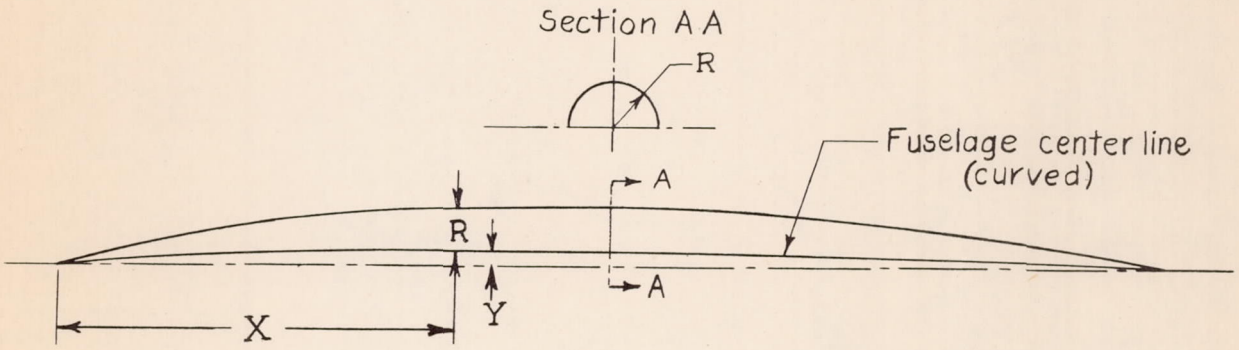

X	Y	R
0	0	0
.070	-----	.032
.105	.006	.042
.175	.011	.060
.350	.022	.101
.700	.042	.169
1.050	.059	.226
1.400	.075	.276
2.100	.102	.363
2.800	.124	.433
3.500	.140	.485
4.200	.153	.524
4.900	.160	.551

X	Y	R
5.600	0.169	0.569
6.300	.177	.580
7.000	.188	.583
7.700	.187	.578
8.400	.181	.563
9.100	.171	.538
9.800	.157	.499
10.500	.140	.438
11.200	.124	.354
11.900	.082	.267
12.600	.064	.178
13.300	.035	.089
14.000	0	0

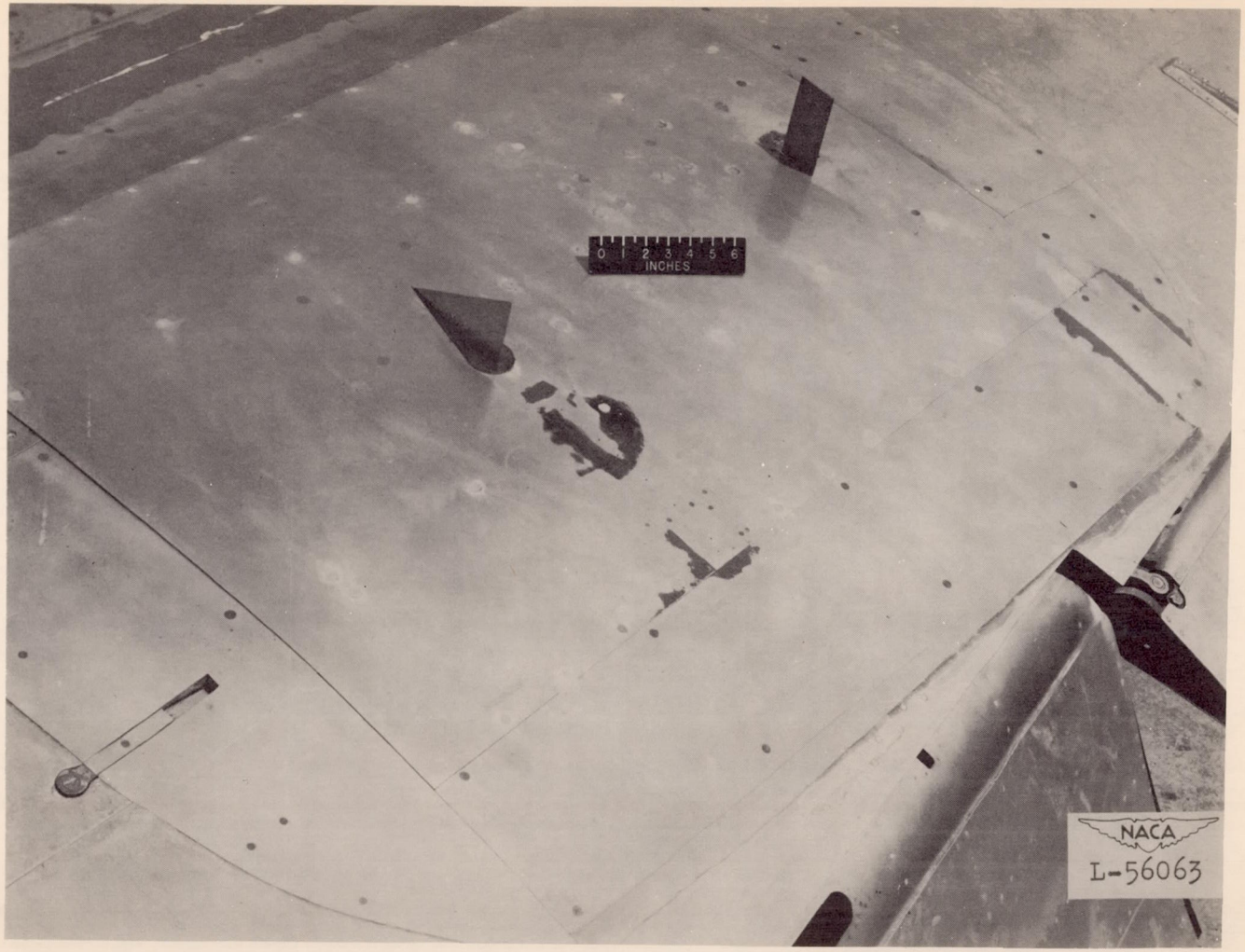

Figure 1.– Semispan wing model shown mounted on wing of F–51D airplane. Free–floating vane is also shown.

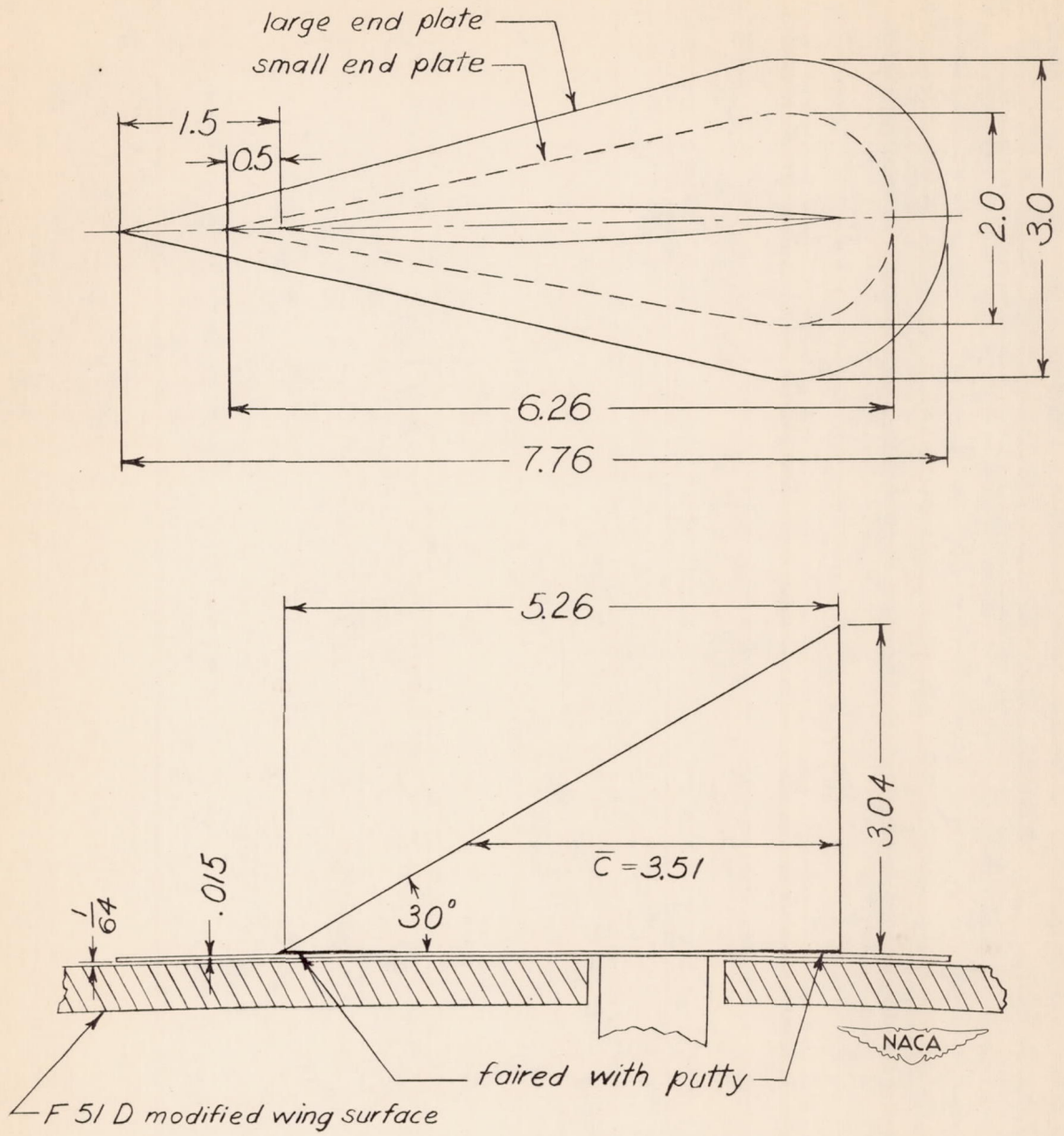

Figure 2.– Details of 6–percent–thick biconvex wing and end plates used in tests of wing alone.

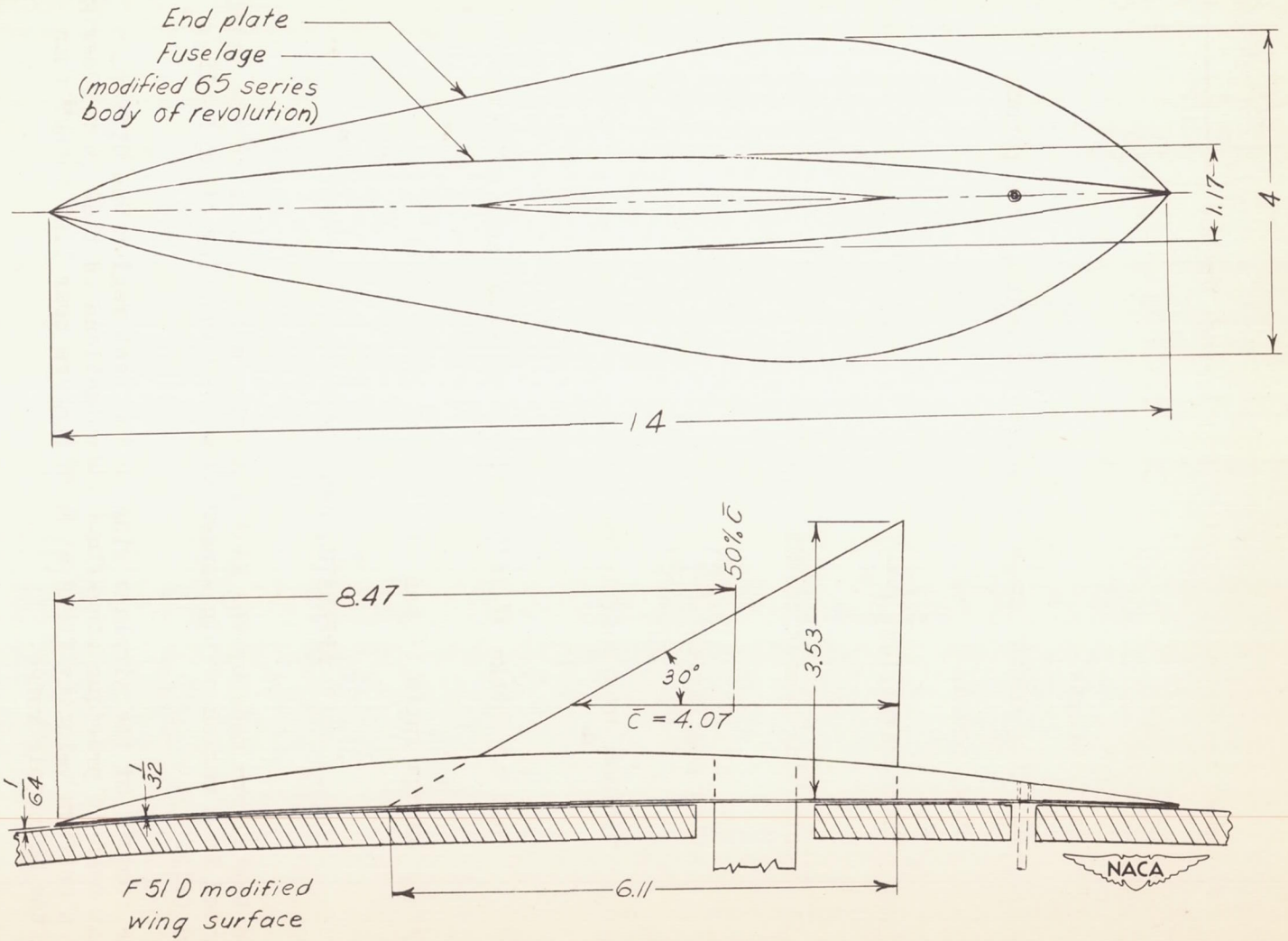

Figure 3.– Details of wing–fuselage model.

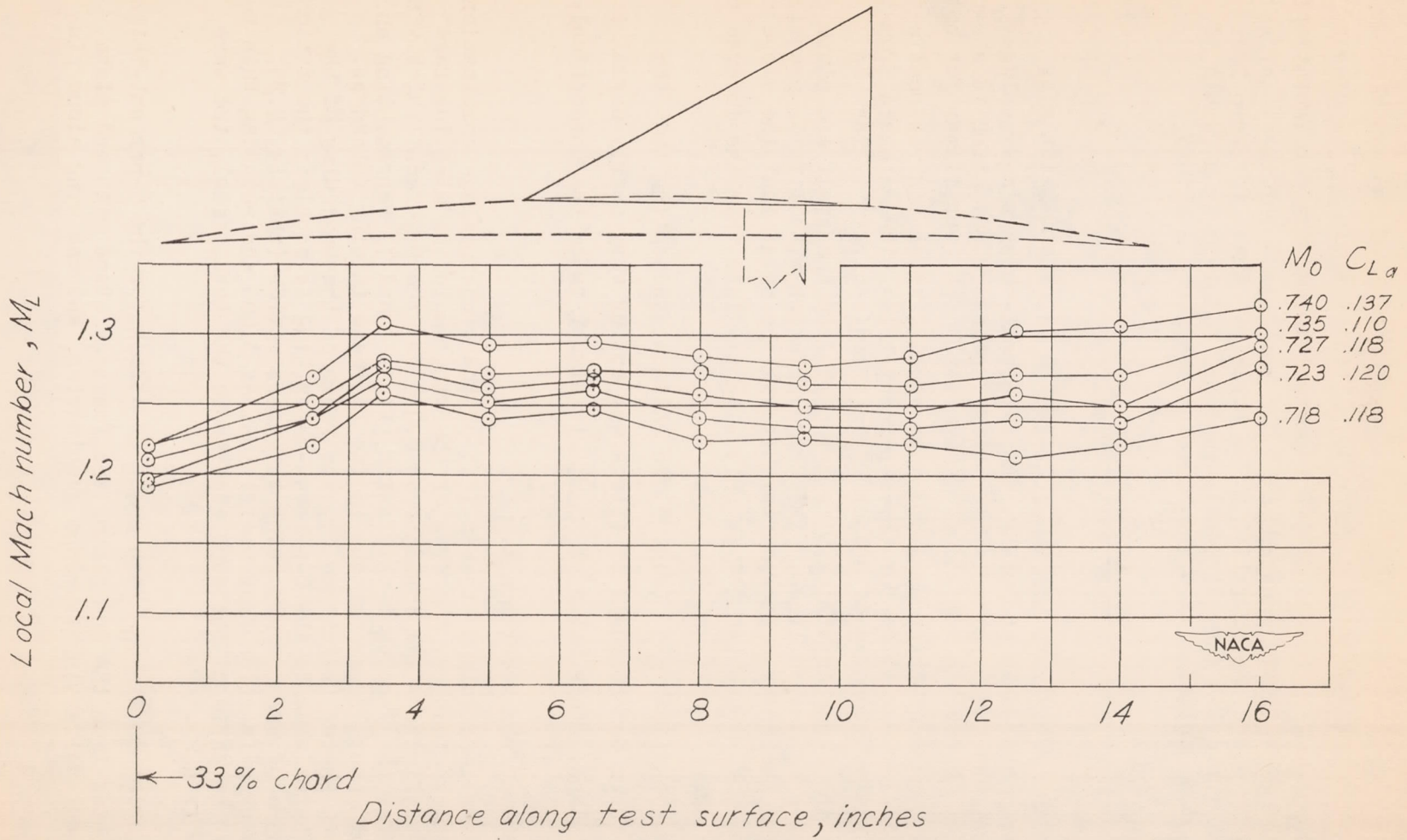

Figure 4.– Typical chordwise local Mach number variation measured at surface of test section. Sketch above curves shows location of model wing alone and wing–fuselage in test region.

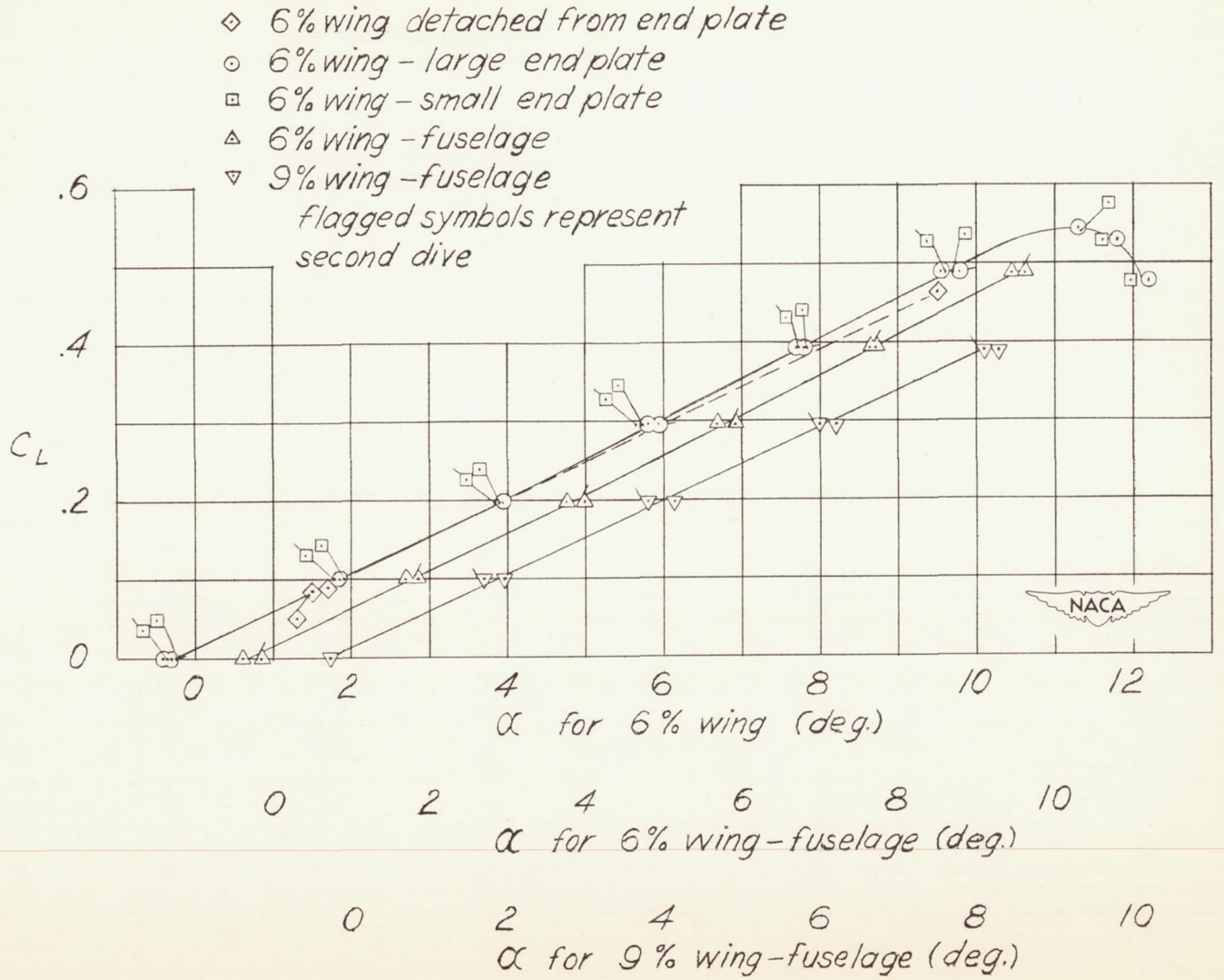

Figure 5.– Variation of lift coefficient with angle of attack for configurations tested. M = 1.25.

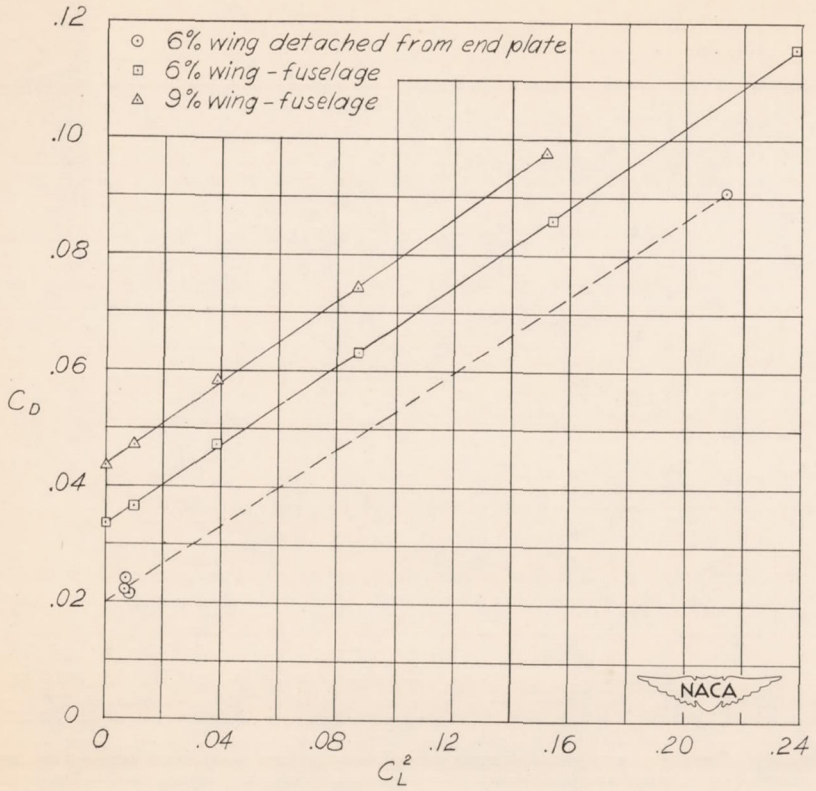

Figure 6.– Variation of drag coefficient with lift coefficient squared at M = 1.25.

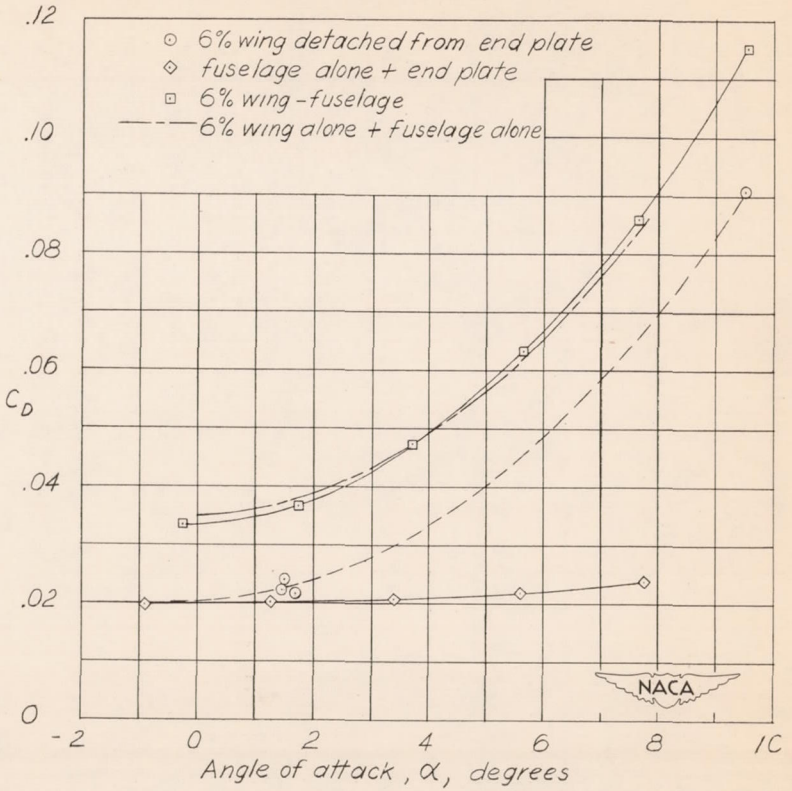

Figure 7.– Variation of drag coefficient with angle of attack at M = 1.25.

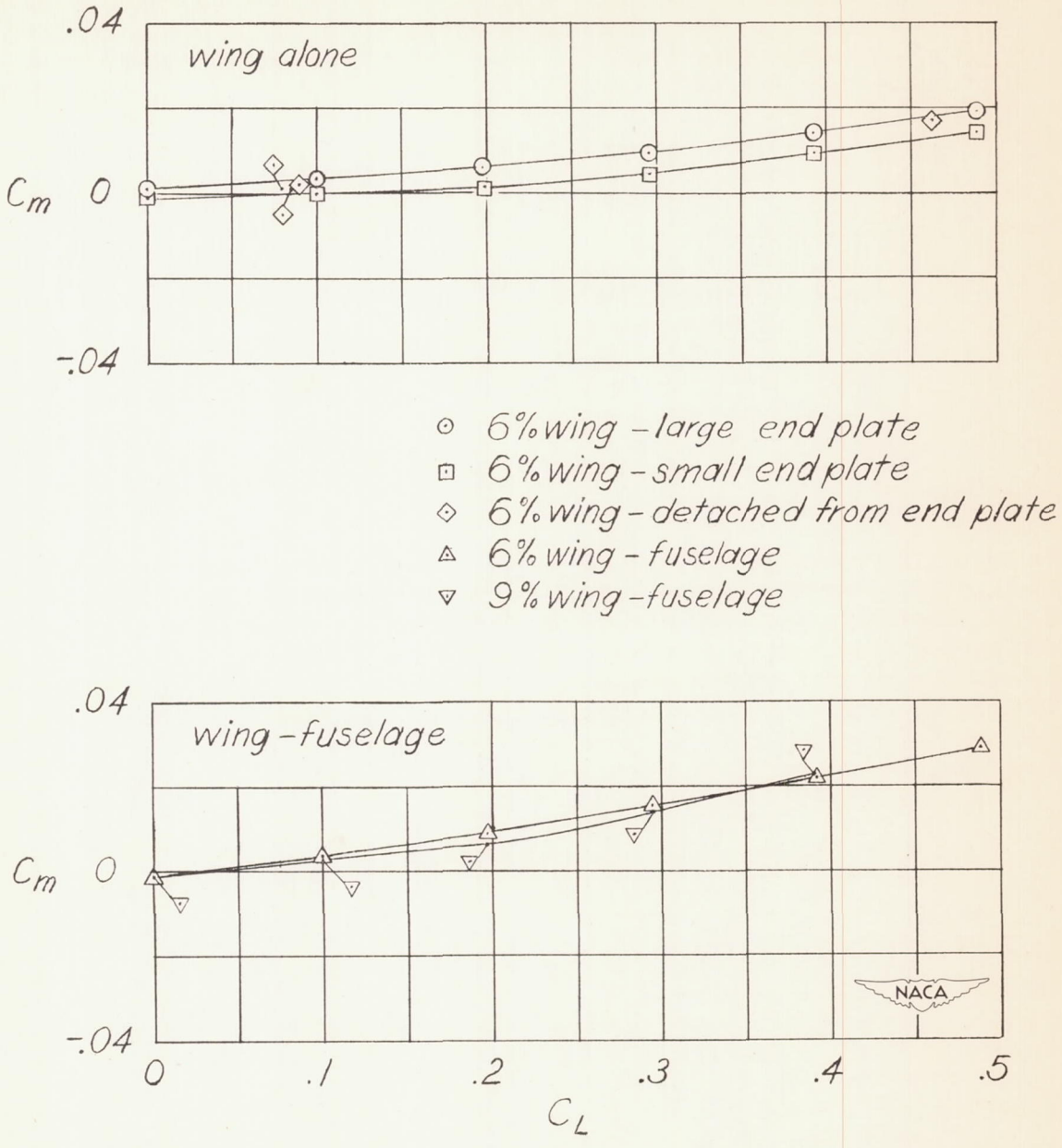

Figure 8.– Variation of pitching-moment coefficient with lift coefficient for the several configurations tested. M = 1.25.

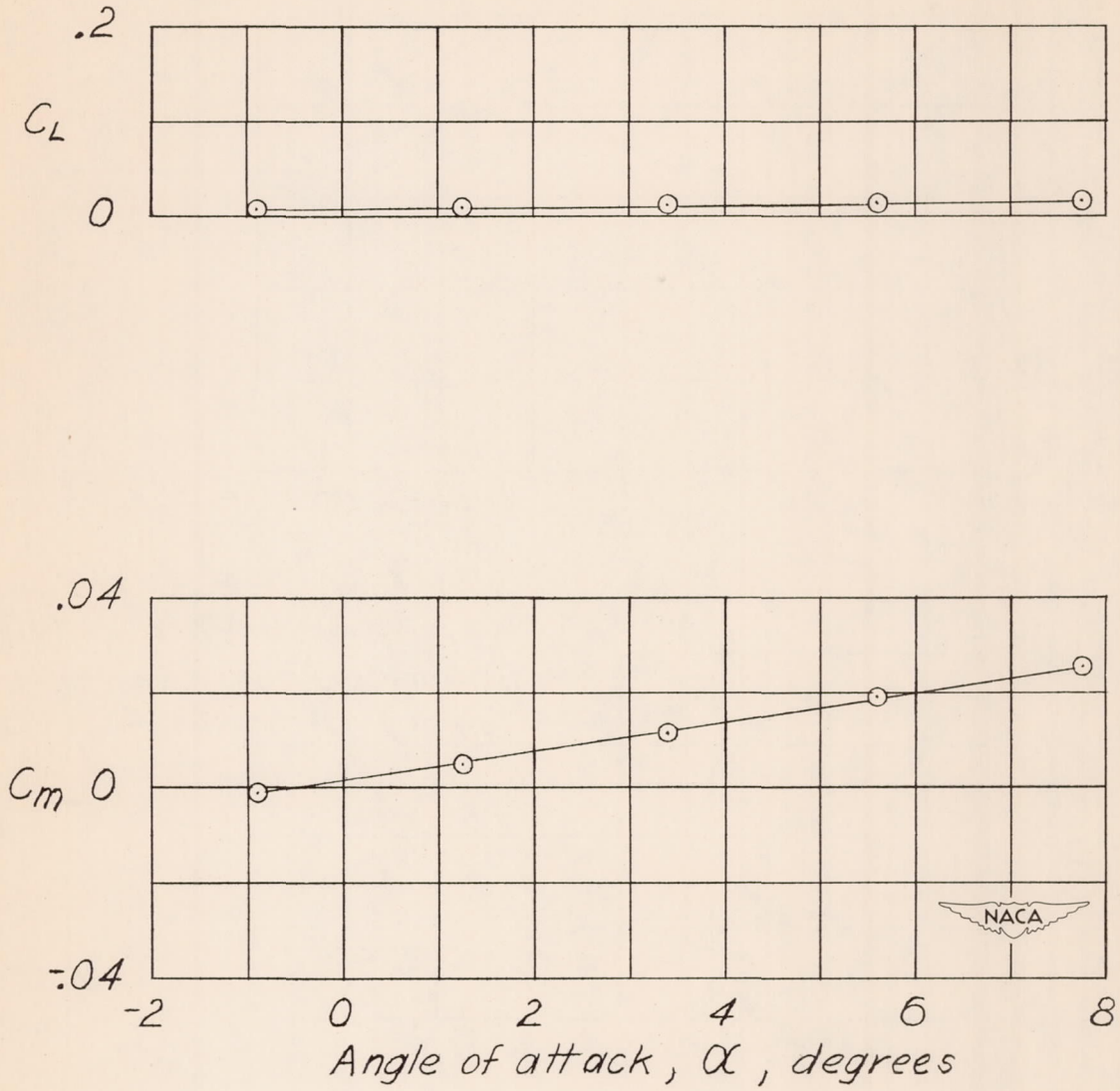

Figure 9.– Variation of lift coefficient and pitching–moment coefficient with angle of attack for the fuselage alone. M = 1.25.

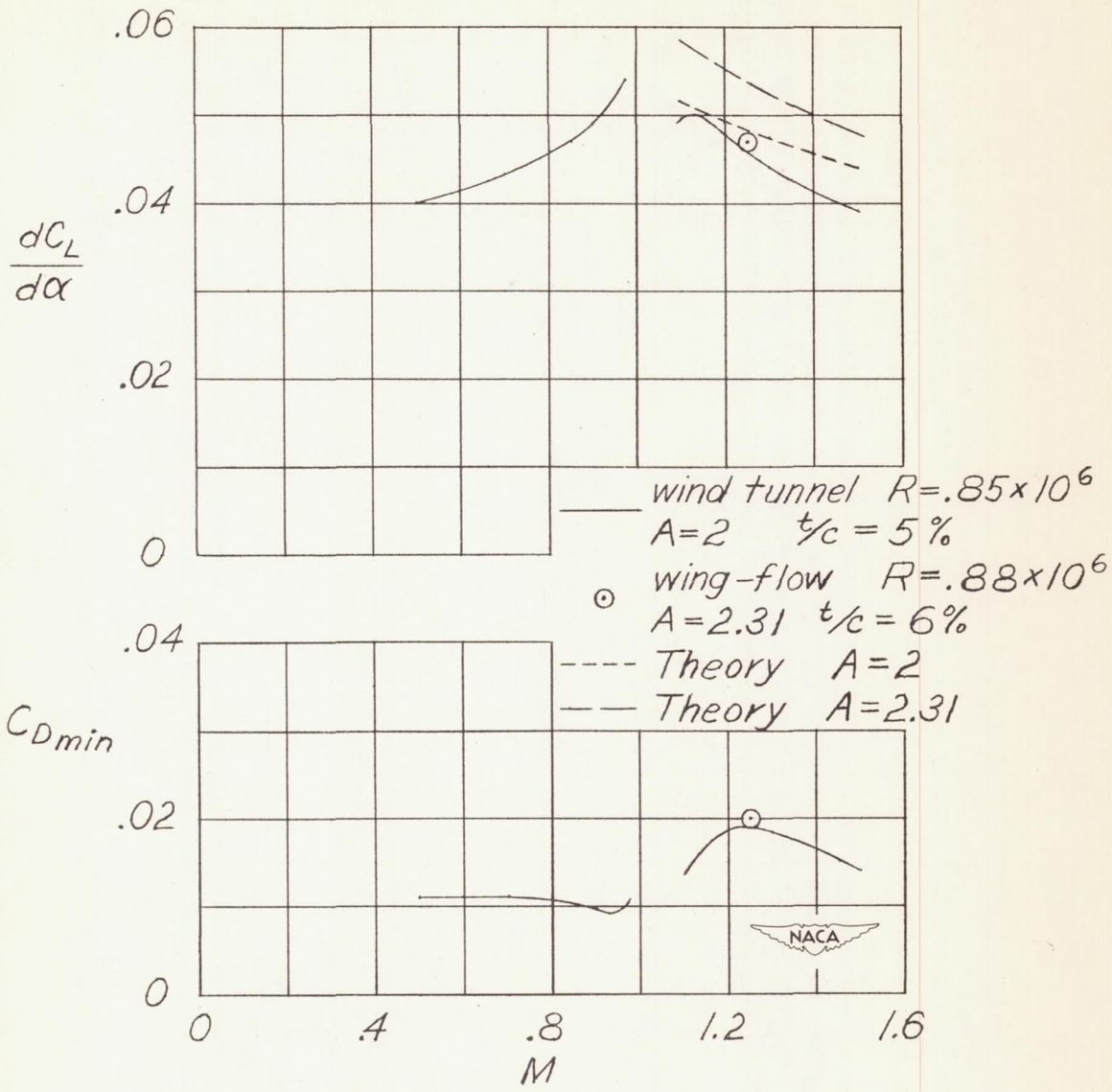

Figure 10.– Comparison of lift–curve slope and minimum drag coefficient for the 6–percent–thick wing alone with some results from reference 3.